Food and Chemical Toxicology 174 (2023) 113669

Contents lists available at ScienceDirect

Food and Chemical Toxicology

journal homepage: www.elsevier.com/locate/foodchemtox

Effect of flavonoids and CYP3A4 variants on midostaurin metabolism

Ren-ai Xu [a,b,1], Qing-qing Li [b,1], Nan-yong Gao [b], Jing Wang [b], Xin-yue Li [b], Feng Ye [b], Jin-huan Ni [b], Guo-xin Hu [b,*], Jian-chang Qian [b,**]

[a] The First Affiliated Hospital of Wenzhou Medical University, Wenzhou, 325000, China
[b] Institute of Molecular Toxicology and Pharmacology, School of Pharmaceutical Sciences, Wenzhou Medical University, Wenzhou, Zhejiang, China

ARTICLE INFO

Handling Editor: Dr. Bryan Delaney

Keywords:
Flavonoids
Midostaurin
CYP3A4
Genetic polymorphism
Myricetin
Interaction

ABSTRACT

The objective of this study was to determine the effect of flavonoids on midostaurin disposition considering co-administration and metabolic enzyme gene polymorphism. Enzymatic incubation assays were performed *in vitro*, while *in vivo* experiments were conducted in Sprague–Dawley rats. The analytes were determined via UPLC-MS/MS. We found that myricetin was the most potent among the investigated 10 flavonoids in suppressing the metabolism of midostaurin, with an IC_{50} at a low μM level. After co-administration of midostaurin and myricetin, the plasma concentration of midostaurin's primary metabolite CGP62221 was reduced corresponding to myricetin exposure. Furthermore, CYP3A4 homologous rat protein CYP3A2 was reduced significantly in the co-administration group. Thereafter, the kinetic parameters of 23 recombinant human CYP3A4 variants were determined using midostaurin. The relative intrinsic clearance varied from 269.63% in CYP3A4.29–8.95% in CYP3A4.17. In addition, the inhibitory potency of myricetin was substantially different for CYP3A4.29 and CYP3A4.17 compared with wild type, with IC_{50} values of 9.85 ± 0.27 μM and 90.99 ± 16.13 μM, respectively. Collectively, our data demonstrated that flavonoids, particularly myricetin, can inhibit the metabolism of midostaurin. Additionally, CYP3A4 genetic polymorphism may contribute to stratification of midostaurin blood exposure.

1. Introduction

Flavonoids are widespread natural substances that are abundant in food and herbs. According to their chemical structure, they can be divided into flavones, flavonols, flavanols, flavanones, anthocyanidins, and isoflavonoids (Li et al., 2018). Due to their diverse biological activities, flavonoids have become a research hot spot. There is growing body of data showing that flavonoids can interact with many drugs (for example, the interactions between myricetin and atomoxetine (Lan et al., 2017), quercetin and repaglinide (Kim et al., 2021), and apigenin and venlafaxine (Zhan et al., 2015)). Therefore, we need to be more cautious when combining flavonoids and drug therapy in clinical practice to consider potential drug efficacy changes.

Midostaurin is a first-generation FMS-like tyrosine kinase 3 inhibitor (Yin et al., 2008). It was approved on April 28, 2017, for the treatment of FLT3-mutant acute myeloid leukemia (Stansfield and Pollyea, 2017). Adverse reactions during the treatment with midostaurin include gastrointestinal toxicities, QTc extension, and interstitial lung disease (Abbas et al., 2019). According to related literature reports, the plasma exposure of midostaurin increases sharply by 6.1-fold when combining midostaurin and ketoconazole (Gu et al., 2018). In contrast, when co-administering midostaurin and rifampin, the blood concentration of midostaurin decreases by 94% (Gu et al., 2018). The efficacy stratification of the clinical drug is not only affected by drug-drug interactions (DDIs), but may also be impacted by the genetic polymorphism of metabolic enzymes. Midostaurin is a substrate of CYP3A4 and is primarily metabolized into CGP52421 and CGP62221 by hepatic CYP3A4 (Yin et al., 2008). However, many physiological factors and pathological conditions can affect the expression and function of CYP3A4 (Congiu et al., 2009; Harvey and Morgan, 2014; Zhang et al., 2011). In particular, genetic polymorphism may increase the clinical manifestations of adverse drug reactions through the changed catalytic reaction of CYP3A4.

In this study, we screened the interaction between midostaurin and 10 flavonoids, particularly myricetin. In addition, based on the novel

* Corresponding author. School of Pharmaceutical Sciences, Wenzhou Medical University, Wenzhou, 325035, China.
** Corresponding author. School of Pharmaceutical Sciences, Wenzhou Medical University, Wenzhou, 325035, China.
E-mail addresses: hgx@wmu.edu.cn (G.-x. Hu), qianjc@wmu.edu.cn (J.-c. Qian).
[1] These authors contributed equally to the work.

https://doi.org/10.1016/j.fct.2023.113669
Received 5 December 2022; Received in revised form 8 February 2023; Accepted 13 February 2023
Available online 17 February 2023

Abbreviations

AML	Acute myeloid leukemia
AUC	area under the blood concentration–time curve
CL_{int}	intrinsic clearance
$CL_{z/F}$	blood clearance
C_{max}	maximum blood concentration
CMC-Na	carboxymethylcellulose sodium salt
CO	carbon monoxide
CYP450	cytochrome P450
CYP3A4	cytochrome P450 3A4
DAS	Drug and statistics
DDIs	drug-drug interactions
FLT3	FMS-like tyrosine kinase 3
HLMs	human liver microsomes
IC_{50}	half-maximal inhibitory concentration
IS	internal standard
K_i	inhibition constant
K_m	Michaelis-Menten constant
LDS	lithium dodecyl sulfate
MRM	multiple reaction monitoring
NADPH	reduced nicotinamide adenine dinucleotide phosphate
OPF	open reading frame
PBS	phosphate buffered saline
PCR	polymerase chain reaction
QTc	Q-T interval
RLMs	rat liver microsomes
S.D.	standard deviation
SD	Sprague-Dawley
$t_{1/2z}$	elimination half time
TDI	time-dependent inhibition
T_{max}	peak time
UPLC-MS/MS	ultra-performance liquid chromatography–tandem mass spectrometry
UV	ultraviolet wavelength
V_{max}	maximum velocity of the reaction
$V_{z/F}$	apparent volume of distribution

recombinant human CYP3A4 variants discovered in previous studies (Supplementary Table S1) (Hu et al., 2017), we explored the enzymatic kinetic characteristics of midostaurin and its metabolites. The results may help promote the clinical individualized precision therapy of midostaurin and provide better medication service for patients.

2. Materials and methods

2.1. Chemical drugs and reagents

Midostaurin was provided by Qisong Biotechnology Co., Ltd (Beijing, China). CGP52421 and CGP62221 were provided by Bailingwei Technology Co., Ltd (Beijing, China). Flavonoids (myricetin, quercetin, apigenin, wogonin, kaempferol, genistein, silibinin, calycosin, baicalin, and baicalein) were purchased from Shanghai Chuangsai Technology Co., Ltd. (Shanghai, China). Diazepam was purchased from Beijing Sunflower Technology Development Co., Ltd. (Beijing, China) and used as internal standard (IS). Pooled rat liver microsomes (RLMs) and human liver microsomes (HLMs) were purchased from Corning Life Sciences Co., Ltd. Recombinant human CYP3A4 and cytochrome *b*5 were prepared by our team (Fang et al., 2017). Reduced nicotinamide adenine dinucleotide phosphate (NADPH) was purchased from Roche Pharmaceutical Ltd. (Basel, Switzerland). All other solvents and chemicals used were of analytical grade.

2.2. Ultra-high performance liquid chromatography tandem mass spectrometry (UPLC-MS/MS) condition

A Waters Acquity ultra-performance liquid chromatography (UPLC) system (Milford, MA, USA) equipped with an Acquity BEH C18 column (2.1 mm × 50 mm, 1.7 μm; Milford, MA, USA) was used to detect the concentrations of midostaurin, CGP52421, CGP62221, and myricetin. Its column temperature was maintained at 40 °C.

The mobile phases of gradient elution were 0.1% formic acid (solvent A) and acetonitrile (solvent B) with a flow rate of 0.40 mL/min. The elution process was as follows: 90% A from 0 to 0.5 min; 90%–10% A from 0.5 to 1.0 min; 10% A from 1.0 to 2.0 min; 10%–90% A from 2.0 to 2.1 min, and 90% A from 2.1 to 3.0 min. The whole process of analysis took 3.0 min. The temperature of the auto-sampler was set at 4 °C, and the injection volume was 2.0 μL for each running process. Quantification was performed using a Waters XEVO TQD triple quadruple mass spectrometer, and the analytes were detected by multiple reaction monitoring (MRM) in positive mode. The ion transitions of midostaurin, CGP52421, CGP62221, myricetin, and IS were m/z 571.20 > 348.10, m/z 587.40 > 363.87, m/z 557.09 > 245.89, m/z 318.94 > 152.88, and m/z 284.91 > 153.90, respectively.

2.3. Preparation of rat/human liver microsomes

Liver was weighed and homogenized by adding 0.01 mM cold phosphate-buffered saline (PBS) containing 0.25 mM sucrose. The homogenate was centrifuged at 10 000 × *g* for 30 min. Then, the supernatant was transferred to a new tube and centrifuged at 10 000 × *g* for 30 min. Next, the supernatant was centrifuged at 10 000 × *g* for 1 h, and the precipitate was resuspended with 0.01 mM cold PBS. Finally, Pierce™ BCA protein assay kit (Thermo Scientific) was used to determine the protein concentration (Wang et al., 2015).

2.4. Preparation of recombinant human CYP3A4 enzyme

The construction of expression vectors, expression of recombinant human CYP3A4 variant, and determination of protein concentration and protein expression level were carried out in line with the previous procedures of our team (Fang et al., 2017). We used the dual-expression baculovirus vector pFastBac Dual, constructed the open-reading frame (ORF) fragments of each CYP3A4 variant through the overlap extension polymerase chain reaction (PCR) amplification, and finally obtained the dual-expression vector pFastBac-OR-CYP3A4. The constructed plasmid was confirmed by sequencing with CEQ DTCS rapid Start Kit (Beckman Coulter, Inc, Brea, CA, USA) and transfected into Sf21 insect cells in SF-900 ™III SFM insect culture medium containing 4 μg/mL heme to obtain recombinant baculovirus. Finally, a Pierce™ BCA protein assay kit (Thermo Scientific) and carbon monoxide (CO) difference spectra were used to determine the protein concentration and protein expression level of recombinant CYP3A4 enzyme, respectively.

2.5. Enzymatic reaction assay

The 200-μL incubation system included 1 M PBS, 1 pmol CYP3A4.1 or other CYP3A4 variants, 50 μg/mL cytochrome *b*5, 1 mM NADPH, and 0.05–2 μM midostaurin. To determine the Cl_{int} (K_m/V_{max}) of different polymorphic enzymes, the concentration of midostaurin was set at 0.05, 0.1, 0.2, 0.5, 1, and 2 μM. We used GraphPad Prism 6.0 software to obtain the K_m of different polymorphic enzymes. Meanwhile, the corresponding V_{max} was expressed in pmol of analyte/min/pmol amount of CYP3A4. Then, we investigated the half-maximum inhibitory

concentration (IC_{50}) of myricetin in CYP3A4.29, CYP3A4.1, CYP3A4.17, with the concentration of myricetin set at 0, 0.01, 0.1, 1, 10, 25, and 50 μM, and the concentration of midostaurin set at 0.5 μM (the corresponding Michaelis–Menten constant value). The mixture was pre-incubated at 37 °C for 5 min before addition of 1 mM NADPH to initiate the reaction. After 30 min of incubation, the reaction was terminated by immediate freezing to −80 °C. Then, 400 μL acetonitrile and 20 μL diazepam (IS, 200 ng/mL) were added to the frozen mixture. After complete melting, the mixture was vortexed fully for 2 min and centrifuged at 13 000 rpm for 10 min. Finally, we took 100 μL of the supernatant for UPLC-MS/MS analysis.

To explore the DDIs *in vitro*, the enzymatic reaction was conducted which contained 1 M PBS, 0.2 mg/mL RLMs or HLMs, 1 mM NADPH, 10 kinds of flavonoids (100 μM), and midostaurin (0.5 μM) to a final volume of 200 μL. To ensure the accuracy of the results for drugs with an inhibition rate ≥80%, we repeated the results by other independent experiments. To determine IC_{50} of myricetin in RLMs or HLMs, the concentration of myricetin was set at 0, 0.01, 0.1, 1, 10, 25, 50, and 100 μM, and midostaurin concentration was set at 0.5 μM. To examine the potential mechanism of myricetin's effect on midostaurin, according to the value of IC_{50}, the concentration of myricetin was set at 0, 0.5, 1, 2, and 4 μM in RLMs and 0, 1.25, 2.5, 5, and 10 μM in HLMs; according to the corresponding Michaelis–Menten constant value, the concentration of midostaurin was set at 0.125, 0.25, 0.5, and 1 μM. First, we used GraphPad Prism 6.0 software to draw the Lineweaver–Burk plot of midostaurin, and then we made secondary plots according to its slope (K_m/V_{max} versus inhibitor concentration) and the y-intercepts ($1/V_{max}$ versus inhibitor concentration) to obtain the inhibition constant (K_i) and αK_i, respectively. To study the time-dependent inhibition, the concentration of myricetin was varied from 0 to 100 μM with or without 1 mM NADPH for 30 min at 37 °C. Thereafter, midostaurin (0.5 μM, the corresponding Michaelis–Menten constant value) was added to the mixture and incubated for another 30 min. The subsequent processing steps were the same as those in the experiments mentioned above.

2.6. Animal experiment

Fifteen Sprague–Dawley rats (250 ± 20 g, purchased from the Shanghai Animal Experimental Center) were randomly divided into the following three groups (n = 5): group A, midostaurin (9 mg/kg, p.o.); group B, myricetin (50 mg/kg, p.o.) and midostaurin (9 mg/kg, p.o.); group C, myricetin (10 mg/kg, i.p.) and midostaurin (9 mg/kg, p.o.). Before the formal experiment, the rats were fasted for 12 h, but were allowed to drink water freely. At the beginning of the experiment, myricetin (50 mg/kg, dissolved in oil) was administered orally in group B, and myricetin (10 mg/kg, dissolved in Tween-80/absolute ethanol/0.9% sodium chloride solution = 1:1:8, v/v/v) was intraperitoneally injected in group C. Thirty minutes later, all groups received midostaurin orally (9 mg/kg, suspended in 0.5% carboxymethylcellulose sodium salt). Blood samples were collected from the tail vein at 1, 2, 3, 4, 5, 6, 8, 10, 12, and 24 h after oral administration of midostaurin. For the preparation of plasma samples, 150 μL acetonitrile and 20 μL diazepam (IS, 200 ng/mL) were added to 50 μL of plasma. After being fully vortexed and centrifuged, the supernatant was obtained for UPLC-MS/MS detection and analysis.

Next, to explore the inhibitory effect of myricetin on CYP3A2 in RLMs, we randomly divided six Sprague–Dawley rats into the following two groups (n = 3): group E, the control group; group F, myricetin (10 mg/kg, dissolved in Tween-80/absolute ethanol/0.9% sodium chloride solution = 1:1:8, v/v/v) injected intraperitoneally. According to the pharmacokinetic results, when the concentration of myricetin reached the maximum in plasma, we extracted the liver tissue of the two groups of Sprague–Dawley rats. Next, the extracted livers were prepared into liver microsomes.

2.7. Immunoblotting assay

First, the liver samples were denatured by mixing with lithium dodecyl sulfate buffer (ThermoFisher, Waltham, MA, USA). Next, 10 μg of the sample was loaded into 10% polyacrylamide gel. After separation, it was electrically transferred to polyvinylidene fluoride membrane. Western blotting was then performed with CYP3A2 antibody. Finally, the protein bands were visualized and imaged using an enhanced chemiluminescence kit.

2.8. Carbon monoxide difference spectra to determine the protein expression level

The differential spectra of the microsomes were measured using a UV–visible spectrophotometer (Thermo Scientific, Waltham, MA, USA) and a 1-cm optical path test tube (Fang et al., 2017). First, the microsomes were diluted in PBS to 1 mg/mL; about 1 mL of the microsomes were then placed into a 2-mL centrifuge tube to which CO gas was introduced for 120 s. Then, we added 5 mg sodium dithionite powder for reduction. After 2 min, the total amount of CYP450 of the microsomes was calculated by measuring the absorbance of the microsomes at 450-nm and 490-nm UV wavelengths.

2.9. Statistical analysis

Experimental data were presented as mean ± standard deviation (S.D.). The Michaelis–Menten, IC50, Lineweaver–Burk plot, and the average plasma concentration–time curves were created using GraphPad Prism 6.0 software. Pharmacokinetic parameters were calculated by non-compartmental analysis using Drug and Statistics (DAS) software (version 3.0, Bontz Inc., Beijing, China). The parameters of CYP3A4.1 and other variants were compared through one-way ANOVA Dunnett's test (SPSS Inc., Chicago, IL, USA), and the kinetic parameters between different groups were compared by unpaired *t*-test. When the statistical result was $P < 0.05$, it was considered statistically significant.

3. Results

3.1. Mass spectrometry and chromatographic characterization of analytes determined by UPLC-MS/MS

The liquid-chromatography results are shown in Supplementary Fig. S1. The retention times of metabolites and diazepam (IS) were 1.61 and 1.68 min, respectively. The standard calibration curves of midostaurin and metabolites were in the range of 0.01–50 ng/mL, and the lower limits of the quantification of midostaurin and metabolites were 0.01 ng/mL.

3.2. Identification of myricetin's potent inhibition of midostaurin metabolism

Fig. 1B and C shows the inhibitory effect of 10 different flavonoids (Fig. 1A) on midostaurin metabolism. According to the results, myricetin (100 μM) achieved 98.88% inhibition. Therefore, we next investigated the inhibitory potency and mode. The IC_{50} of myricetin in RLMs and HLMs was 1.69 ± 0.96 μM and 5.55 ± 0. 45 μM, respectively, as shown in Fig. 1D and E. Then, we determined enzyme kinetics. The results demonstrated that myricetin took a mixed mechanism in RLMs, with a $K_i = 4.82$ μM and $\alpha K_i = 2.14$ μM (Fig. 2A); however, myricetin showed an uncompetitive mechanism in HLMs, with a $\alpha K_i = 4.05$ μM (Fig. 2B). In addition, the IC_{50} shift assay was used to detect time-dependent inhibition (TDI). As shown in Fig. 2C, the $IC_{50(-NADPH)} : IC_{50(+NADPH)}$ ratio was 0.56. Based on the research of Stresser and Mao, a ratio ("shift") of >1.3 is often used to classify a compound as a time-dependent inhibitor. Thus, myricetin was not a time-dependent inhibitor of midostaurin in RLMs (Stresser et al., 2014).

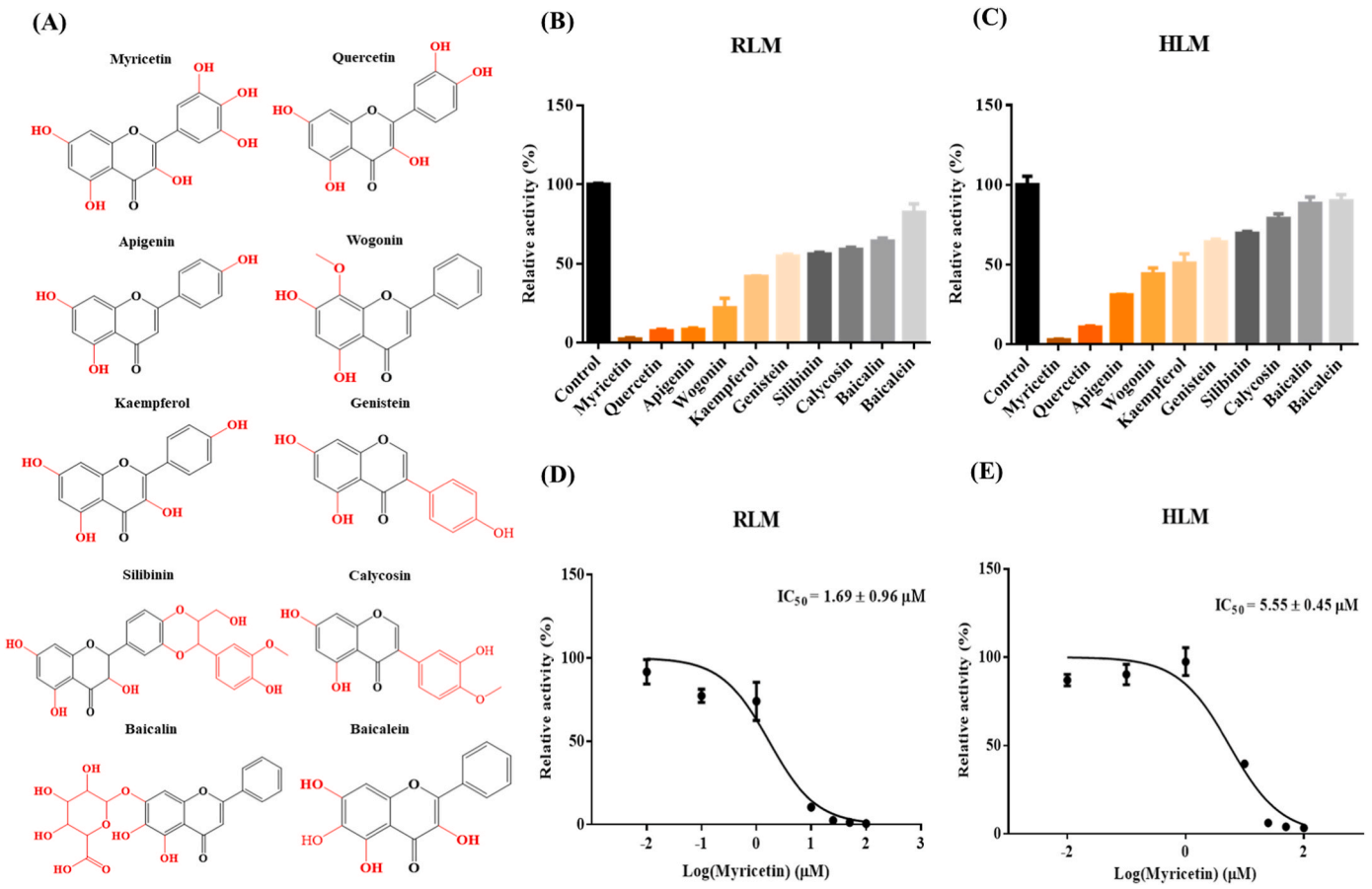

Fig. 1. Screening for flavonoids that may interact with midostaurin. (A) The structure of 10 flavonoids in this study. (B)–(C) Inhibitory effect of flavonoids (100 μM) on the metabolism of midostaurin in RLMs (B) and HLMs (C), respectively. (E)–(F) The half-maximum inhibitory concentration (IC_{50}) of myricetin in RLMs (E) and HLMs (F), respectively. Data are presented as the means ± S.D.

3.3. Myricetin significantly reduces the drug exposure of CGP62221 in rats

Fig. 3A–C shows the average concentration–time curves of CGP62221, CGP52421, and midostaurin, and Tables 1–3 show the corresponding pharmacokinetic parameters. Compared with group A (midostaurin, 9 mg/kg, p.o.), group B (myricetin, 50 mg/kg, p.o. + midostaurin, 9 mg/kg, p.o.) showed no significant differences in pharmacokinetic parameters of CGP62221, CGP52421, and midostaurin. However, the $AUC_{(0\text{-}t)}$ of midostaurin in group C (myricetin, 10 mg/kg, i.p. + midostaurin, 9 mg/kg, p.o.) decreased by about 2.38-fold, while $AUC_{(0\text{-}t)}$ of CGP62221 in group C (myricetin, 10 mg/kg, i.p. + midostaurin, 9 mg/kg, p.o.) was significantly reduced to 51.45%. Moreover, as shown in Fig. 3D, compared with group B, the blood concentration of myricetin in group C was significantly higher, indicating that the administration of intraperitoneal injection had made the absorption of myricetin more complete.

Next, we investigated the effect of myricetin on the liver. As shown in Fig. 4A–C, the total amount of CYP450 in RLMs (isolated from livers of the rats in group E and group F) decreased significantly after administration of myricetin. At the same time, according to Fig. 4E, myricetin significantly reduced the expression of CYP3A2 in RLMs (isolated from livers of the rats in group E and group F), which may be attributed to the significant decrease in CYP450 abundance.

3.4. The catalytic activity of recombinant human CYP3A4 as evaluated by midostaurin metabolism

In this study, midostaurin was used as a substrate to verify the catalytic activity of CYP3A4.1 and other 23 variants, and the intrinsic clearance (CL_{int}) was considered to assess the enzyme activity of each variant. Fig. 5 and Table 4 show the Michaelis–Menten curve and the Michaelis kinetic parameters of midostaurin after metabolism by wild-type CYP3A4.1 and other variants. According to Table 4, there were two main situations for the change in the maximum velocity of the reaction (V_{max}): compared with CYP3A4.1, CYP3A4.4, .5, .7, .8, .10, .12, .13, .14, .15, .16, .17, .18, .19, .20, .23, .28, .31, .32, and .34 showed a decrease in V_{max}, ranging from 6.53% to 87.04%; while CYP3A4.2, .3, .29, .33 were significantly increased in V_{max}, ranging from 126.29% to 236.03%. There were two main changes in K_m value: compared with CYP3A4.1, CYP3A4.29 showed no significant difference (no change); CYP3A4.2 and CYP3A4.3 showed an increased K_m, ranging from 147.75% to 189.71%; and the other variants showed significantly reduced K_m, ranging from 22.33% to 92.75%. There were also three categories in CL_{int} value as follows: compared with CYP3A4.1, CYP3A4.2, .14, .18, and .34 showed no significant difference; CYP3A4.4, .5, .10, .15, .16, .19, .23, .28, .29, .31, .32, and .33 showed a marked increase, with CL_{int} ranging from 101.61% to 253.31%; the other variants showed a decrease, with CL_{int} ranging from 10.54% to 95.75%. To further study the influence of CYP3A4 variants on myricetin's inhibitory efficacy, the IC_{50} values of myricetin in CYP3A4.29, CYP3A4.1, and CYP3A4.17 were determined. They were 9.85 ± 0.27 μM, 4.44 ± 0.12 μM, and 90.99 ± 16.13 μM respectively, as shown in Fig. 5E–G.

4. Discussion

Acute myeloid leukemia (AML), a clonal hematopoietic disease that affects hematopoietic stem and progenitor cells, is the most common

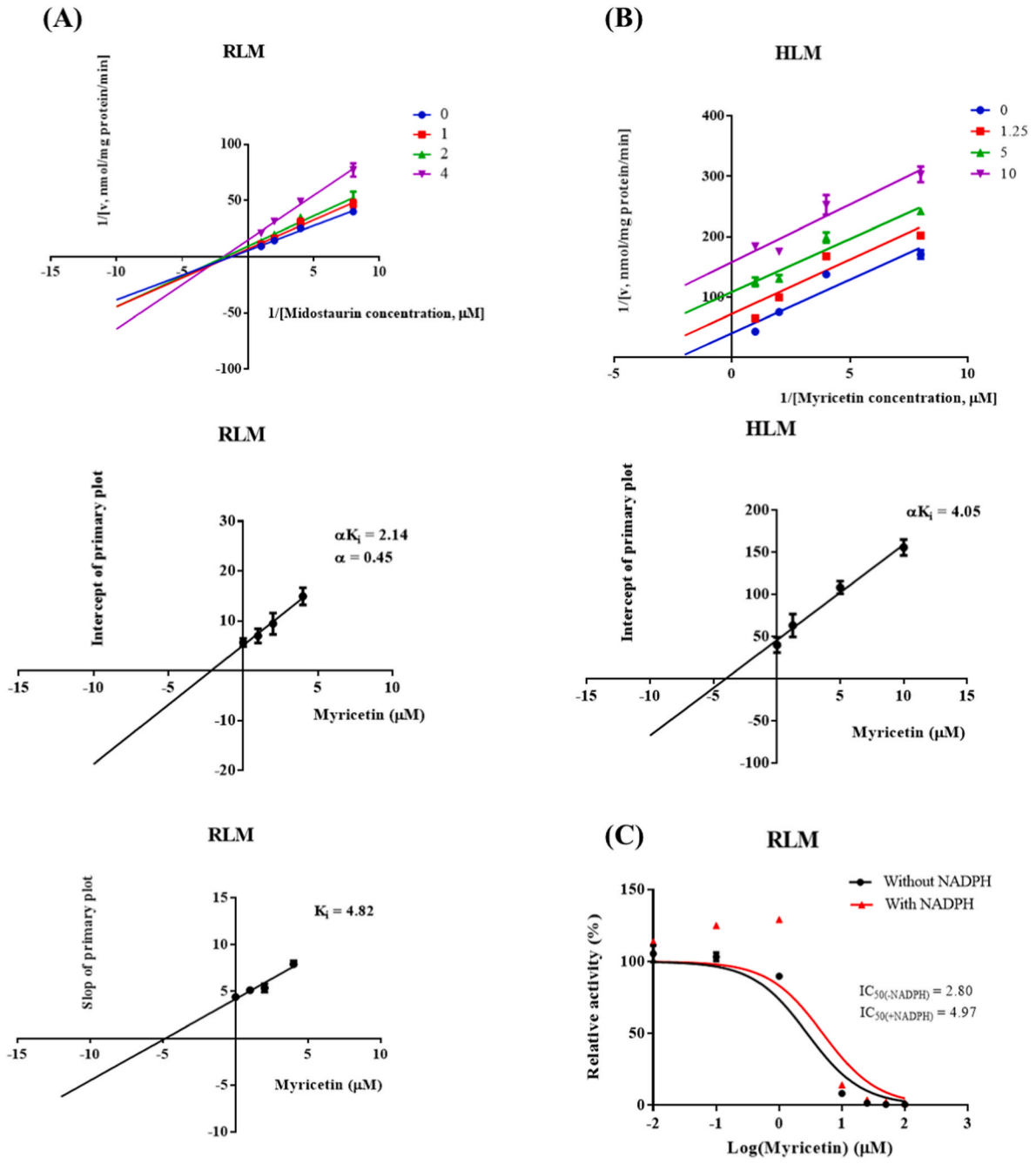

Fig. 2. The potential mechanism of myricetin's effect on midostaurin. (A) Lineweaver–Burk plot, the secondary plot for αK_i, and the secondary plot for K_i in the inhibition of midostaurin metabolism by myricetin with various concentrations in RLMs. (B) Lineweaver–Burk plot and the secondary plot for αK_i in the inhibition of midostaurin metabolism by myricetin with various concentrations in HLMs. (C) The inhibition curves of myricetin in RLMs with or without NADPH. Data are presented as the means ± S.D.; n = 3.

acute leukemia in adults (its median age at diagnosis is 67 years) (Ferrara and Schiffer, 2013; Siegel et al., 2017); however, the prognosis of patients with FLT3 mutation is poor (Stansfield and Pollyea, 2017). Midostaurin, a multitarget kinase inhibitor for the treatment of newly diagnosed FLT3-mutant AML (Kim, 2017), has been shown to significantly improve overall survival in AML patients (Stansfield and Pollyea, 2017; Yin et al., 2008). However, some adverse reactions of midostaurin can occur during treatment, such as gastrointestinal toxicities, corrected Q-T interval (QTc) extension, and interstitial lung disease (Abbas et al., 2019). The efficacy of midostaurin shows obvious individual differences, and variation of drug blood exposure may be one of the reasons. Genetic polymorphisms of metabolic enzymes and DDIs often affect drug blood concentrations.

Midostaurin is mainly metabolized by CYP3A4 into CGP52421 and CGP62221 in the liver (Yin et al., 2008). Hence, we used CGP52421 (the incubation response value of CGP62221 was too low) as an analyte to investigate the influence of CYP3A4 genetic polymorphism on disposition of midostaurin. *In vitro*, the catalytic activity of CYP3A4.3, CYP3A4.7, CYP3A4.8, CYP3A4.12, CYP3A4.13, CYP3A4.17, CYP3A4.20, and CYP3A4.34 variants was significantly lower than that of CYP3A4.1, which may be due to the premature stop codons and generation of truncated proteins (Zhou et al., 2011). Meanwhile, many variants (CYP3A4.4, .5, .10, .15, .16, .19, .23, .28, .29, .31, .32, .33) showed a higher catalytic activity than CYP3A4.1. Among them, the

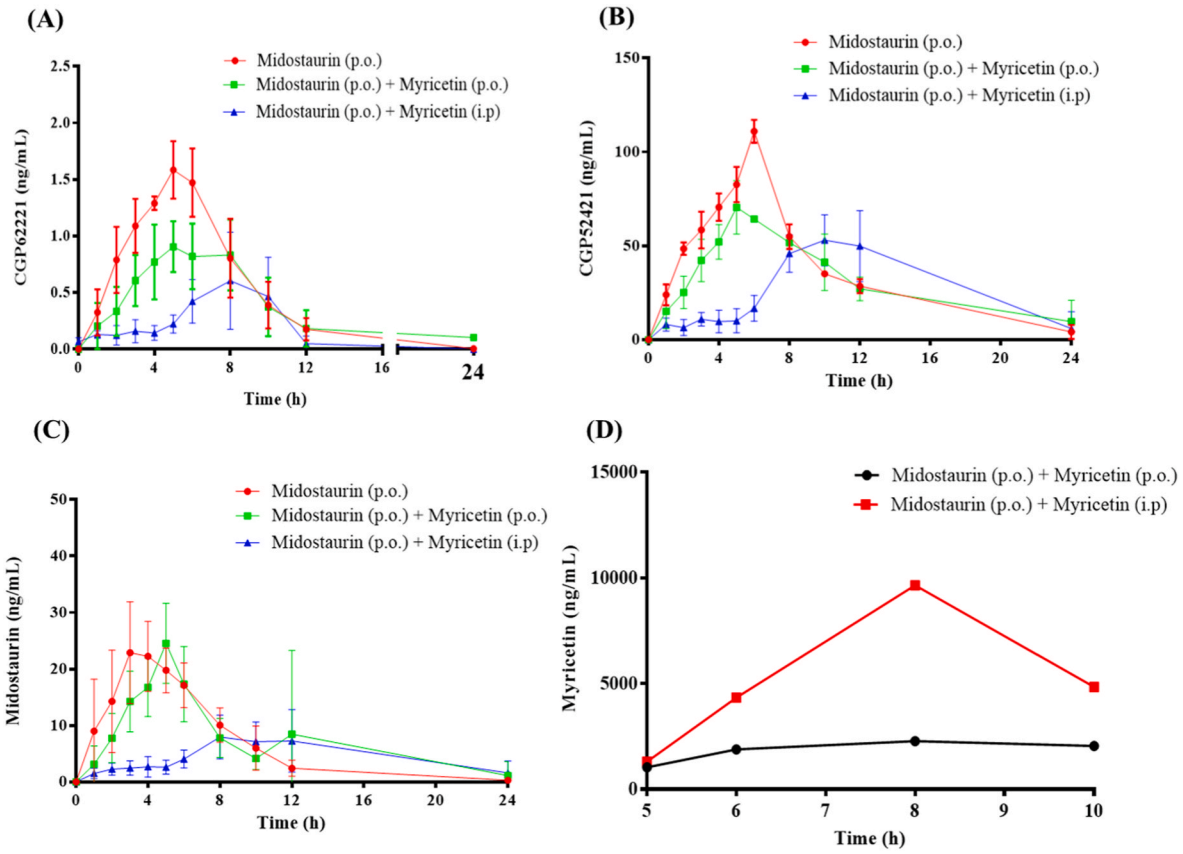

Fig. 3. Effect of myricetin on midostaurin *in vivo*. (A) The average concentration–time curves of CGP62221 in three groups. (B) The average concentration–time curves of CGP52421 in three groups. (C) The average concentration–time curves of midostaurin in three groups. Data are presented as the means ± S.D.; n = 5. (D) The blood concentration of myricetin in two groups. Data are presented as the means.
(A)–(C) Compared with group A, the plasma exposure of CGP62221 and midostaurin was significantly lower in group C; nevertheless, there was no significant difference relative to group B. In addition, the plasma exposure of CGP52421 was almost the same in the three groups. (D) The plasma concentration of myricetin in group B was lower than that in group C.

Table 1
Main pharmacokinetic parameters of CGP62221 in three groups of rats (n = 5).

Parameters	Midostaurin (9 mg/kg, p.o.)	Midostaurin (9 mg/kg, p.o.) + Myricetin (50 mg/kg, p.o.)	Midostaurin (9 mg/kg, p.o.) + Myricetin (10 mg/kg, i.p.)
$AUC_{(0-t)}$ (ng/mL*h)	9.30 ± 1.25	6.87 ± 2.83	4.51 ± 2.48 *
$AUC_{(0-\infty)}$ (ng/mL*h)	11.27 ± 2.87	15.55 ± 13.21	8.54 ± 5.62
$t_{1/2z}$ (h)	9.24 ± 6.41	34.20 ± 60.45	3.79 ± 3.65
T_{max} (h)	4.40 ± 0.89	3.80 ± 1.64	8.80 ± 3.03 *
$V_{z/F}$ (L/kg)	9860.68 ± 4733.40	16417.92 ± 18656.3	7530.88 ± 5748.44
$CL_{z/F}$ (L/h/kg)	845.27 ± 231.25	807.04 ± 349.44	1665.76 ± 1263.77
C_{max} (ng/mL)	1.04 ± 0.20	0.78 ± 0.41	0.67 ± 0.37

Notes: AUC, area under the blood concentration–time curve; $t_{1/2z}$, elimination half time; T_{max}, peak time; $V_{z/F}$, apparent volume of distribution; $CL_{z/F}$, blood clearance; C_{max}, maximum blood concentration. *P < 0.05, compared with the control group.

Table 2
Main pharmacokinetic parameters of CGP52421 in three groups of rats (n = 5).

Parameters	Midostaurin (9 mg/kg, p.o.)	Midostaurin (9 mg/kg, p.o.) + Myricetin (50 mg/kg, p.o.)	Midostaurin (9 mg/kg, p.o.) + Myricetin (10 mg/kg, i.p.)
$AUC_{(0-t)}$ (ng/mL*h)	620.90 ± 161.08	459.52 ± 229.38	583.37 ± 166.16
$AUC_{(0-\infty)}$ (ng/mL*h)	627.08 ± 166.62	482.13 ± 212.02	1196.09 ± 1147.35
$t_{1/2z}$ (h)	2.83 ± 0.79	2.62 ± 0.32	8.38 ± 7.86
T_{max} (h)	4.40 ± 1.14	5.20 ± 0.45	12.4 ± 6.70
$V_{z/F}$ (L/kg)	59.48 ± 9.22	81.65 ± 37.12	99.86 ± 83.83
$CL_{z/F}$ (L/h/kg)	15.45 ± 5.28	21.53 ± 8.38	12.00 ± 6.72
C_{max} (ng/mL)	73.16 ± 21.40	62.94 ± 23.04	48.93 ± 17.82

Notes: AUC, area under the blood concentration–time curve; $t_{1/2z}$, elimination half time; T_{max}, peak time; $V_{z/F}$, apparent volume of distribution; $CL_{z/F}$, blood clearance; C_{max}, maximum blood concentration. *P < 0.05, compared with the control group.

V_{max} values of CYP3A4.2, CYP3A4.3, CYP3A4.29, and CYP3A4.33 variants were significantly increased, which may be the main reason for the increase in their catalytic activity, while the K_m value of the other variants was significantly decreased, which may be the primary reason for the increase in their catalytic activity. Moreover, the catalytic activity of other CYP3A4 variants (CYP3A4.2, .14, .18, .34) was similar to that of CYP3A4.1 without significant difference. Although the clinical relevance of CYP3A4 genotype and metabolic phenotype is still under discussion, existing data demonstrated that the median trough concentration of tacrolimus in *CYP3A4*22* (rs35599367) carrier was observably higher than that of *CYP3A4*1/*1* at the third month post-transplantation (Ebid et al., 2022). In short, CYP3A4 genetic polymorphism may impact the metabolism of midostaurin to different degrees. Thus, it may be advantageous to further explore the impact of

Table 3
Main pharmacokinetic parameters of midostaurin in three groups of rats (n = 5).

Parameters	Midostaurin (9 mg/kg, p.o.)	Midostaurin (9 mg/kg, p.o.) + Myricetin (50 mg/kg, p.o.)	Midostaurin (9 mg/kg, p.o.) + Myricetin (10 mg/kg, i.p.)
$AUC_{(0-t)}$ (ng/mL*h)	155.48 ± 53.35	106.83 ± 154.63	65.21 ± 20.70 **
$AUC_{(0-\infty)}$ (ng/mL*h)	162.03 ± 51.90	321.93 ± 293.79	96.94 ± 47.96
$t_{1/2z}$ (h)	2.34 ± 1.04	4.74 ± 7.50	4.51 ± 2.76
T_{max} (h)	3.60 ± 1.34	3.60 ± 0.55	7.60 ± 2.19 **
$V_{z/F}$ (L/kg)	190.47 ± 63.33	162.52 ± 107.12	608.85 ± 186.62 ***
$CL_{z/F}$ (L/h/kg)	60.22 ± 18.71	51.96 ± 39.46	108.37 ± 41.18
C_{max} (ng/mL)	25.14 ± 4.78	40.80 ± 21.52	8.77 ± 2.85 ***

Notes: AUC, area under the blood concentration–time curve; $t_{1/2z}$, elimination half time; T_{max}, peak time; $V_{z/F}$, apparent volume of distribution; $CL_{z/F}$, blood clearance; C_{max}, maximum blood concentration. **P < 0.01, ***P < 0.001, compared with the control group.

CYP3A4 polymorphisms on exposure to midostaurin in AML patients.

Flavonoids are natural substances that are widely found in our daily foods and herbal medicines, such as fruits, vegetables, tea, and soybeans (Aherne and O'Brien, 2002; Higdon and Frei, 2003; Kalaiselvan et al., 2010; Lopez-Lazaro, 2009). They have anti-inflammatory, antibacterial, anticancer, antilipidemic, antihyperglycemic, and other biological activities (Cazarolli et al., 2008; Cushnie and Lamb, 2011; Friedman, 2007; Wang et al., 2014; Woo and Kim, 2013). At present, people prefer using natural products to synthetic drugs to enhance physical fitness. Flavonoids show little toxicity and are consumed in large quantities in our daily life (Li et al., 2018). As flavonoids are often used by patients as dietary supplements, food additives, and medicines, increasing attention should be paid to their drug interactions. In this study, we systematically screened 10 flavonoids to determine the effect of DDIs on midostaurin metabolism. We found that myricetin (100 μM) achieved 98.88% inhibition. Modern pharmacological studies have shown that myricetin has a variety of biological activities, such as anti-inflammatory (Hou et al., 2018), antitumor (Jiang et al., 2019; Stoll et al., 2019), antibacterial (Jiang et al., 2020), and cardioprotective activities (Wang et al., 2019); thus, it is widely used as food additive. It may be possible to administer myricetin during clinical treatment of patients with AML. In this study, we mainly explored the effect of myricetin on midostaurin metabolism. According to our results, myricetin is not a time-independent inhibitor of midostaurin. It is worth noting that myricetin has different potential inhibitory mechanisms. For example, myricetin showed a mixed inhibitory mechanism in RLMs, with a K_i = 4.82 μM and αK_i = 2.14 μM, and an uncompetitive inhibitory mechanism in HLMs, with an αK_i = 4.05 μM. As shown in our *in vivo* experiment from the variation in the blood concentration of myricetin between group B and group C, intraperitoneal administration resulted in increased the exposure of myricetin more than oral administration did. Meanwhile, compared with a single oral dose of midostaurin, the $AUC_{(0-t)}$ of CGP62221 and midostaurin significantly decreased after co-administering an intraperitoneal injection of myricetin and an oral dose of midostaurin. Nevertheless, when co-administering myricetin and midostaurin orally, there was no significant difference in CGP62221 and midostaurin. These observations suggest that different administration methods could affect the absorption of myricetin and that the lower metabolite exposure was due to the lower exposure to midostaurin, which may be related to lower absorption. Thus, myricetin might not have an inhibitory effect solely on CYP3A4 *in vivo*. Indeed, it has been reported that flavonoids affect intestinal peristalsis (Gharzouli and Holzer, 2004). Furthermore, the

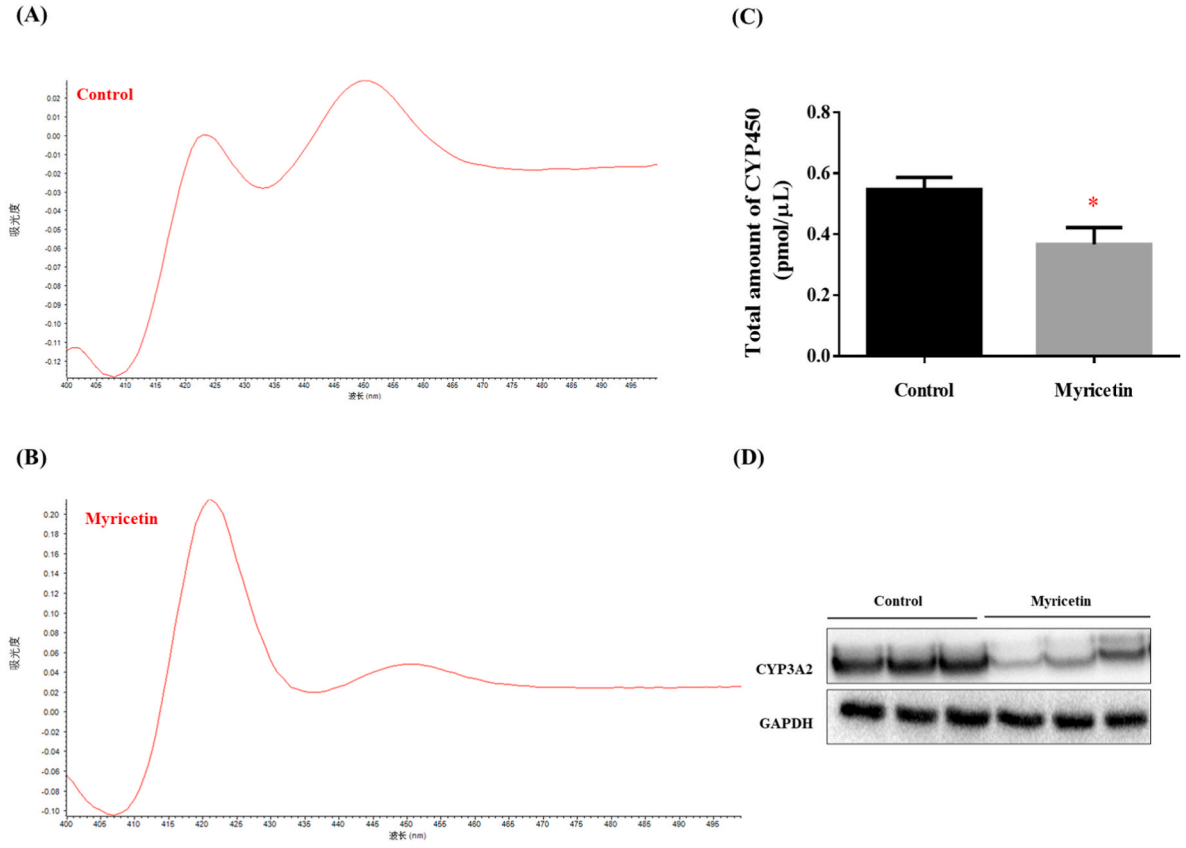

Fig. 4. Effects of myricetin on total amount of CYP450 and CYP3A2 expression in RLMs isolated from livers of the rats in group E and group F. The chromatogram (A–B) and the total amount of CYP450 (C) in RLMs quantified using the CO quantitative method in two groups. The immunoblotted and the gray-scale value of RLMs was quantified (D) in the two groups. Data are presented as the mean ± S.D.; n = 3.

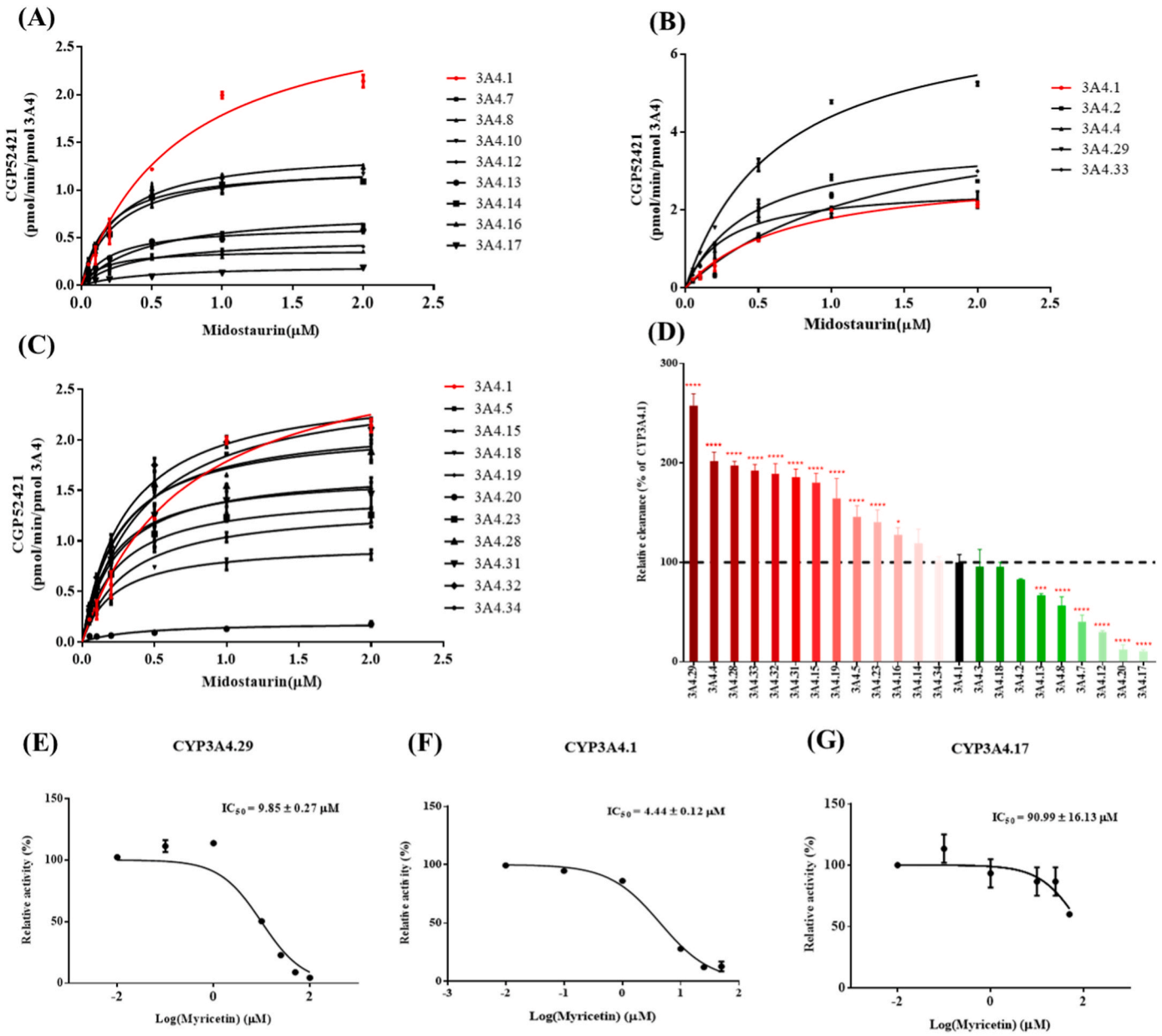

Fig. 5. The Michaelis–Menten curves of the enzymatic activities of the wild-type CYP3A4.1 and other CYP3A4 variants on the metabolism of midostaurin (A)–(C). The relative clearance of CYP3A4 variants toward the metabolism of midostaurin compared with the wild-type CYP3A4.1 (D). The half-maximum inhibitory concentration (IC_{50}) of myricetin in CYP3A4.29 (E), CYP3A4.1 (F), and CYP3A4.17 (G). Data are presented as the means ± S.D.; n = 3. *P < 0.05, **P < 0.01, ***P < 0.001.

results of immunoblotting and CO difference spectra showed that myricetin could inhibit the expression of CYP3A2 and reduce the total amount of CYP450 in RLMs. Mechanistically, the reduction of the drug exposure of CGP62221 in rats was probably due to the remarkable decrease in CYP450 abundance, especially CYP3A2. However, the *in vivo* effect for midostaurin showed the opposite of the expected, and the reason that the plasma exposure to midostaurin decreased when co-administering myricetin and midostaurin needs to be further investigated.

5. Conclusion

Flavonoids can inhibit the metabolism of midostaurin. Attention should be paid when clinically combining the use of midostaurin with flavonoid-enriched nutritional supplements, fruit, or traditional Chinese medicine. In particular, myricetin should be avoided. In addition, CYP3A4 genetic polymorphism may affect midostaurin metabolism, which provides a certain reference for establishing genotype–phenotype relationships in clinical drug application.

CRediT authorship contribution statement

Ren-ai Xu: Conceptualization, Formal analysis, Visualization, Funding acquisition, Writing – original draft, Writing – review & editing, Resources, Data curation. **Qing-qing Li:** Conceptualization, Formal analysis, Visualization, Funding acquisition, Writing – original draft, Writing – review & editing. **Nan-yong Gao:** Methodology, Investigation, Formal analysis, Data curation, Visualization. **Jing Wang:** Methodology, Investigation. **Xin-yue Li:** Investigation, Data curation. **Feng Ye:** Writing – original draft, Writing – review & editing. **Jin-huan Ni:** Supervision, Writing – original draft. **Guo-xin Hu:** Funding acquisition, Supervision, Supervision, Writing – original draft, Writing – review &

Table 4
Michaelis kinetic parameters of midostaurin after metabolism of recombinant human CYP3A4.1 and other variants.

Variants	V_{max} (pmol/min/pmol P450)	K_m (μM)	CL_{int} (V_{max}/K_m) (μl/min/pmol P450)
3A4.1	3.026 ± 0.079	0.692 ± 0.063	4.392 ± 0.343
3A4.2	4.770 ± 0.019 ****	1.313 ± 0.016 ****	3.632 ± 0.037
3A4.3	4.191 ± 0.250 ****	1.023 ± 0.220 ****	4.205 ± 0.754 ****
3A4.4	2.634 ± 0.293 **	0.298 ± 0.042 ****	8.871 ± 0.393 ****
3A4.5	2.593 ± 0.147 ***	0.408 ± 0.054 ***	6.398 ± 0.487 ****
3A4.7	0.809 ± 0.074 ****	0.473 ± 0.123 ****	1.763 ± 0.299 ****
3A4.8	0.376 ± 0.026 ****	0.155 ± 0.034 ****	2.485 ± 0.380 ****
3A4.10	1.239 ± 0.010 ****	0.187 ± 0.016 ****	6.669 ± 0.540 ****
3A4.12	0.495 ± 0.042 ****	0.381 ± 0.052 ****	1.306 ± 0.068 ****
3A4.13	0.627 ± 0.032 ****	0.213 ± 0.016 ****	2.942 ± 0.066 ***
3A4.14	1.278 ± 0.043 ****	0.246 ± 0.021 ****	5.224 ± 0.632
3A4.15	2.329 ± 0.263 ****	0.296 ± 0.046 ****	7.917 ± 0.407 ****
3A4.16	1.424 ± 0.029 ****	0.255 ± 0.018 ****	5.605 ± 0.316 *
3A4.17	0.214 ± 0.029 ****	0.475 ± 0.124 *	0.463 ± 0.070 ****
3A4.18	0.956 ± 0.053 ****	0.228 ± 0.004 ****	4.194 ± 0.0.199
3A4.19	1.723 ± 0.079 ****	0.241 ± 0.025 ****	7.210 ± 0.895 ****
3A4.20	0.198 ± 0.044 ****	0.409 ± 0.193 ***	0.546 ± 0.203 ****
3A4.23	1.480 ± 0.080 ****	0.242 ± 0.035 ****	6.161 ± 0.541 ****
3A4.28	2.146 ± 0.138 ****	0.247 ± 0.017 ****	8.680 ± 0.175 ****
3A4.29	7.202 ± 0.158 ****	0.637 ± 0.041	11.321 ± 0.521 ****
3A4.31	1.668 ± 0.082 ****	0.205 ± 0.018 ****	8.166 ± 0.348 ****
3A4.32	2.624 ± 0.108 ***	0.316 ± 0.015 ****	8.312 ± 0.443 ****
3A4.33	3.822 ± 0.145 ****	0.453 ± 0.029 **	8.447 ± 0.273 ****
3A4.34	1.348 ± 0.061 ****	0.303 ± 0.025 ****	4.463 ± 0.181

Notes: Compared with CYP3A4.1, *P < 0.05, **P < 0.01, ***P < 0.001, ****P < 0.0001. ND, not determined.

editing. **Jian-chang Qian:** Conceptualization, Supervision, Project administration, Funding acquisition, Writing – original draft, Writing – review & editing.

Declaration of competing interest

The authors declare that they have no known competing financial interests or personal relationships that could have appeared to influence the work reported in this paper.

Data availability

Data will be made available on request.

Acknowledgments and Funding

This work was supported by the National Key Research and Development Program of China (2020YFC2008301), the National Natural Science Foundation of China (81973397), and the Natural Science Foundation of Zhejiang Province (LTGC23H310001). We thank the Scientific Research Center of Wenzhou Medical University for their consultation and for providing us with the use of their instruments to support this work. We thank LetPub (www.letpub.com) for its linguistic assistance during the preparation of this manuscript.

Appendix A. Supplementary data

Supplementary data to this article can be found online at https://doi.org/10.1016/j.fct.2023.113669.

References

Abbas, H.A., Alfayez, M., Kadia, T., Ravandi-Kashani, F., Daver, N., 2019. Midostaurin in acute myeloid leukemia: an evidence-based review and patient selection. Cancer Manag. Res. 11, 8817–8828.
Aherne, S.A., O'Brien, N.M., 2002. Dietary flavonols: chemistry, food content, and metabolism. Nutrition 18, 75–81.
Cazarolli, L.H., Zanatta, L., Alberton, E.H., Figueiredo, M.S., Folador, P., Damazio, R.G., Pizzolatti, M.G., Silva, F.R., 2008. Flavonoids: prospective drug candidates. Mini Rev. Med. Chem. 8, 1429–1440.
Congiu, M., Mashford, M.L., Slavin, J.L., Desmond, P.V., 2009. Coordinate regulation of metabolic enzymes and transporters by nuclear transcription factors in human liver disease. J. Gastroenterol. Hepatol. 24, 1038–1044.
Cushnie, T.P., Lamb, A.J., 2011. Recent advances in understanding the antibacterial properties of flavonoids. Int. J. Antimicrob. Agents 38, 99–107.
Ebid, A.I.M., Ismail, D.A., Lotfy, N.M., Mahmoud, M.A., M, E.L., 2022. Influence of CYP3A4*22 and CYP3A5*3 combined genotypes on tacrolimus dose requirements in Egyptian renal transplant patients. J. Clin. Pharm. Therapeut. 47, 2255–2263.
Fang, P., Tang, P.F., Xu, R.A., Zheng, X., Wen, J., Bao, S.S., Cai, J.P., Hu, G.X., 2017. Functional assessment of CYP3A4 allelic variants on lidocaine metabolism in vitro. Drug Des. Dev. Ther. 11, 3503–3510.
Ferrara, F., Schiffer, C.A., 2013. Acute myeloid leukaemia in adults. Lancet 381, 484–495.
Friedman, M., 2007. Overview of antibacterial, antitoxin, antiviral, and antifungal activities of tea flavonoids and teas. Mol. Nutr. Food Res. 51, 116–134.
Gharzouli, K., Holzer, P., 2004. Inhibition of Guinea pig intestinal peristalsis by the flavonoids quercetin, naringenin, apigenin and genistein. Pharmacology 70, 5–14.
Gu, H., Dutreix, C., Rebello, S., Ouatas, T., Wang, L., Chun, D.Y., Einolf, H.J., He, H., 2018. Simultaneous physiologically based pharmacokinetic (PBPK) modeling of parent and active metabolites to investigate complex CYP3A4 drug-drug interaction potential: a case example of midostaurin. Drug Metab. Dispos. 46, 109–121.
Harvey, R.D., Morgan, E.T., 2014. Cancer, inflammation, and therapy: effects on cytochrome p450-mediated drug metabolism and implications for novel immunotherapeutic agents. Clin. Pharmacol. Ther. 96, 449–457.
Higdon, J.V., Frei, B., 2003. Tea catechins and polyphenols: health effects, metabolism, and antioxidant functions. Crit. Rev. Food Sci. Nutr. 43, 89–143.
Hou, W., Hu, S., Su, Z., Wang, Q., Meng, G., Guo, T., Zhang, J., Gao, P., 2018. Myricetin attenuates LPS-induced inflammation in RAW 264.7 macrophages and mouse models. Future Med. Chem. 10, 2253–2264.
Hu, G.X., Dai, D.P., Wang, H., Huang, X.X., Zhou, X.Y., Cai, J., Chen, H., Cai, J.P., 2017. Systematic screening for CYP3A4 genetic polymorphisms in a Han Chinese population. Pharmacogenomics 18, 369–379.
Jiang, M., Zhu, M., Wang, L., Yu, S., 2019. Anti-tumor effects and associated molecular mechanisms of myricetin. Biomed. Pharmacother. 120, 109506.
Jiang, S., Tang, X., Chen, M., He, J., Su, S., Liu, L., He, M., Xue, W., 2020. Design, synthesis and antibacterial activities against Xanthomonas oryzae pv. oryzae, Xanthomonas axonopodis pv. Citri and Ralstonia solanacearum of novel myricetin derivatives containing sulfonamide moiety. Pest Manag. Sci. 76, 853–860.
Kalaiselvan, V., Kalaivani, M., Vijayakumar, A., Sureshkumar, K., Venkateskumar, K., 2010. Current knowledge and future direction of research on soy isoflavones as a therapeutic agents. Pharm. Rev. 4, 111–117.
Kim, E.S., 2017. Midostaurin: first global approval. Drugs 77, 1251–1259.
Kim, J.M., Seo, S.W., Han, D.G., Yun, H., Yoon, I.S., 2021. Assessment of metabolic interaction between repaglinide and quercetin via mixed inhibition in the liver: in vitro and in vivo. Pharmaceutics 13.
Lan, T., Hu, X.X., Liang, B.Q., Pan, W.H., Zhou, Q., Yuan, L.J., Hu, G.X., 2017. The effect of myricetin on pharmacokinetics of atomoxetine and its metabolite 4-hydroxyatomoxetine in vivo and in vitro. Eur. J. Drug Metab. Pharmacokinet. 42, 261–268.
Li, Y., Ning, J., Wang, Y., Wang, C., Sun, C., Huo, X., Yu, Z., Feng, L., Zhang, B., Tian, X., Ma, X., 2018. Drug interaction study of flavonoids toward CYP3A4 and their quantitative structure activity relationship (QSAR) analysis for predicting potential effects. Toxicol. Lett. 294, 27–36.
Lopez-Lazaro, M., 2009. Distribution and biological activities of the flavonoid luteolin. Mini Rev. Med. Chem. 9, 31–59.
Siegel, R.L., Miller, K.D., Jemal, A., 2017. Cancer statistics, 2017. CA A Cancer J. Clin. 67, 7–30.
Stansfield, L.C., Pollyea, D.A., 2017. Midostaurin: a new oral agent targeting FMS-like tyrosine kinase 3-mutant acute myeloid leukemia. Pharmacotherapy 37, 1586–1599.
Stoll, S., Bitencourt, S., Laufer, S., Ines Goettert, M., 2019. Myricetin inhibits panel of kinases implicated in tumorigenesis. Basic Clin. Pharmacol. Toxicol. 125, 3–7.

Stresser, D.M., Mao, J., Kenny, J.R., Jones, B.C., Grime, K., 2014. Exploring concepts of in vitro time-dependent CYP inhibition assays. Expet Opin. Drug Metabol. Toxicol. 10, 157–174.
Wang, L., Wu, H., Yang, F., Dong, W., 2019. The protective effects of myricetin against cardiovascular disease. J. Nutr. Sci. Vitaminol. 65, 470–476.
Wang, X., Ouyang, Y.Y., Liu, J., Zhao, G., 2014. Flavonoid intake and risk of CVD: a systematic review and meta-analysis of prospective cohort studies. Br. J. Nutr. 111, 1–11.
Wang, Z., Sun, W., Huang, C.K., Wang, L., Xia, M.M., Cui, X., Hu, G.X., Wang, Z.S., 2015. Inhibitory effects of curcumin on activity of cytochrome P450 2C9 enzyme in human and 2C11 in rat liver microsomes. Drug Dev. Ind. Pharm. 41, 613–616.
Woo, H.D., Kim, J., 2013. Dietary flavonoid intake and smoking-related cancer risk: a meta-analysis. PLoS One 8, e75604.
Yin, O.Q., Wang, Y., Schran, H., 2008. A mechanism-based population pharmacokinetic model for characterizing time-dependent pharmacokinetics of midostaurin and its metabolites in human subjects. Clin. Pharmacokinet. 47, 807–816.
Zhan, Y.Y., Liang, B.Q., Gu, E.M., Hu, X.X., Lin, D., Hu, G.X., Zheng, Z.Q., 2015. Inhibitory effect of apigenin on pharmacokinetics of venlafaxine in vivo and in vitro. Pharmacology 96, 118–123.
Zhang, Y., Klein, K., Sugathan, A., Nassery, N., Dombkowski, A., Zanger, U.M., Waxman, D.J., 2011. Transcriptional profiling of human liver identifies sex-biased genes associated with polygenic dyslipidemia and coronary artery disease. PLoS One 6, e23506.
Zhou, Q., Yu, X., Shu, C., Cai, Y., Gong, W., Wang, X., Wang, D.M., Hu, S., 2011. Analysis of CYP3A4 genetic polymorphisms in Han Chinese. J. Hum. Genet. 56, 415–422.